Macromolecules

Article

pubs.acs.org/Macromolecules

Structure and Dynamics of Interacting Nanoparticles in Semidilute Polymer Solutions

Ryan Poling-Skutvik,[†] Katrina Irene S. Mongcopa,[†] Antonio Faraone,[§] Suresh Narayanan,[∥] Jacinta C. Conrad,*[,†] and Ramanan Krishnamoorti*[,†,‡]

[†]Department of Chemical and Biomolecular Engineering and [‡]Department of Chemistry, University of Houston, Houston, Texas 77204, United States

[§]National Institute of Standards and Technology Center for Neutron Research, Gaithersburg, Maryland 20899, United States

[∥]Advanced Photon Source, Argonne National Laboratory, Argonne, Illinois 60439, United States

Supporting Information

ABSTRACT: We investigate the structure and dynamics of silica nanoparticles and polymer chains in semidilute solutions of high molecular weight polystyrene in 2-butanone to determine the effect of long-range interparticle interactions on the coupling between particle and polymer dynamics. Particles at concentrations of 1−10 wt % are well dispersed in the semidilute polymer solutions and exhibit long-range electrostatic repulsions between particles. Because the particles are comparably sized to the radius of gyration of the polymer, the particle dynamics is predicted to couple to that of the polymer. We verify that the polymer structure and dynamics are not significantly affected by the particles, indicating that the particle−polymer coupling does not change with increasing particle loading. We find that the coupling between the dynamics of comparably sized particles and polymer results in subdiffusive particle dynamics, as expected. Over the interparticle distance, however, the particle dynamics is hindered and not fully described by the relaxation of the surrounding polymer chains. Instead, the particle dynamics is inversely related to the structure factor, suggesting that physical particle−polymer coupling on short length scales and interparticle interactions on long length scales both present energetic barriers to particle motion that lead to subdiffusive dynamics and de Gennes narrowing, respectively.

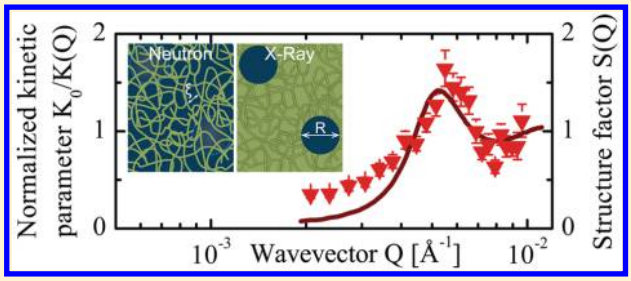

1. INTRODUCTION

Materials containing both nanoparticles and polymers in solid and/or liquid states are important both technologically and scientifically. When dispersed in a polymer matrix, nanoparticles can substantially improve the electrical,[1,2] optical,[3,4] and mechanical performance[5,6] of nanocomposite materials compared to neat polymer melts. Additionally, polymer solutions containing suspended nanoparticles serve as model systems to understand the complex processes governing targeted drug delivery through biological tissues[7,8] and transport through porous media.[9,10] To predict and control material and transport properties, the physics governing the particle dynamics must be well understood. For large particles diffusing in a homogeneous medium, the particle dynamics follows the generalized Stokes−Einstein equation and the diffusivity D is inversely related to bulk viscosity η.[11] When the particle is comparably sized to heterogeneities in solution, however, the particle dynamics deviates from predictions based on bulk solution properties.[12,13]

Heterogeneities exist in polymer solutions over length scales comparable to the polymer radius of gyration R_g and correlation length ξ. When the particle is similarly sized to these length scales, the assumption that the solution is homogeneous fails, and the resulting particle dynamics deviates strongly from Stokes−Einstein behavior.[12] For dilute particle dispersions in semidilute polymer solutions, a nanoparticle of size R is transiently trapped by the surrounding polymer mesh. At short times, the particle dynamics couples to those of the surrounding polymer, resulting in subdiffusive motion.[14] At long times, the polymer mesh fully relaxes and the particle motion becomes diffusive.[15−17] The long-time diffusivity of the particle can be quantitatively described by models that incorporate polymer relaxations over the surface of the particle.[14,18]

As the concentration of particles increases, interparticle interactions lead to structural ordering of the system and hence may significantly change the particle dynamics. For many materials, including nanocomposites[19] and cellular cytoplasm,[20] the nanoparticle concentration commonly exceeds 30 vol %, and the resulting physics is not the same as that in the dilute particle limit. In concentrated systems, de Gennes first showed that fluctuations are suppressed over the characteristic

Received: June 14, 2016
Revised: July 26, 2016
Published: August 17, 2016

DOI: 10.1021/acs.macromol.6b01277
Macromolecules 2016, 49, 6568−6577

structural length scale due to a minimum in the free energy landscape.[21,22] Relaxations out of the free energy minimum are less favorable than those over other length scales, resulting in an inverse relationship between diffusive dynamics and structure. Although this "de Gennes narrowing" has been observed in a variety of non-Newtonian systems, including dense colloidal suspensions with[23] and without[24] charge and colloidal gels,[25] it is not known how interparticle interactions affect particle dynamics when the particles experience a locally heterogeneous environment. Indeed, the relationship between structure and dynamics may depend strongly on the physical interactions with surrounding media, as evidenced by the absence of de Gennes narrowing in a soft micelle system.[26]

Measuring the dynamics of nanoparticles in polymer solutions is experimentally difficult because of the wide range of relevant length and time scales and the presence of multiple mobile species. The particle−polymer coupling derives from relaxations over ξ, whereas the interparticle interactions exist over the interparticle distance $x_{ID} \gg \xi$. Additionally, both the particle and polymer are mobile, requiring independent measurements of both particle and polymer dynamics. Common experimental methods such as microscopy and rheology investigate dynamics over a large range of time and length scales but are limited to probing only a single component or the bulk properties of the solution. Although significant advances have been made in understanding the nanoscale structure and dynamics of complex media using scattering methods,[27,28] the majority of studies focus primarily on a single component within the system. Extending scattering techniques to measure both components independently over the relevant time and length scales requires a model system in which the scattering contrasts between particle, polymer, and solvent are tunable and well controlled.

In this study, we use complementary X-ray and neutron scattering techniques to measure the structure and dynamics of both charged nanoparticles and polymer chains in semidilute solutions of high molecular weight polymer. We independently determine the structure and dynamics of the particles using X-rays and of the polymer using neutrons in the same solutions. This combination of techniques accesses a wide range of time and length scales from 1 ns to 100 s and 1 nm to over 100 nm, respectively, essential to understanding the anomalous dynamics of nanoparticles in polymer solutions. With long-range repulsive interparticle interactions, the particles are well dispersed in the presence of the polymer. The polymer correlation length changes slightly at high polymer concentration because of an increase in excluded volume and the dynamics of the polymer are unaffected by the particles. Using X-ray photon correlation spectroscopy (XPCS), we find the particle dynamics is subdiffusive due to coupling to polymer relaxations. Using neutron spin-echo spectroscopy (NSE), we verify the underlying assumption of the coupling model[14] that the polymer dynamics in semidilute solutions are unperturbed in the presence of nanoparticles. Moreover, the particle dynamics is suppressed at the structure factor peak due to the electrostatic repulsion between particles, consistent with the physics underlying de Gennes narrowing. Together, these results indicate that the interparticle interactions affect particle dynamics on long time and length scales even when the particle dynamics is coupled to those of the polymer on shorter time and length scales. With interparticle interactions and dynamic coupling to polymer relaxations, this system enables future studies on the relationships between structure and dynamics in composite systems and complex fluids.

2. MATERIALS AND METHODS

To prepare the particle−polymer solutions, we first add appropriate quantities of polystyrene of weight-averaged molecular weight M_w = 706 kDa (Polymer Source, Inc., M_w/M_n = 1.06) to either fully protonated 2-butanone (Sigma-Aldrich, ≥99%) or partially deuterated 1,1,1,3,3-d_5-2-butanone (Cambridge Isotope Laboratories, ≥98%).[a] The intrinsic viscosity of PS in 2-butanone follows $[\eta] = 0.039M_w^{0.58}$ and for the 706 kDa PS is calculated to be 93 mL/g.[29] We verify this prediction by measuring the intrinsic viscosity of our polymer in dilute solutions using a capillary viscometer to be 104 ± 12 mL/g (Supporting Information, Figure S1), in agreement with predictions. Using standard relations,[30] we calculate the overlap concentration $c^* = 1/[\eta]$ and approximate the radius of gyration[31] in dilute solution $R_{g,0} \approx [M_w/(4/3\pi N_{av}c^*)]^{1/3}$ to be 10.7 g/L and 29 nm, respectively.

The polystyrene and 2-butanone solutions homogenize for 3−4 days on a roller, after which time we add the appropriate amount of silica nanoparticles (Nissan Chemical America, ≈30 wt % silica in 2-butanone, $R \approx 25$ nm). The silica particles are obtained as stable dispersions in 2-butanone. For fully protonated solutions, the particles are used as received. For partially deuterated solutions, the silica particles are dried overnight in vacuum to remove solvent and then resuspended in d_5-2-butanone and sonicated before mixing with polystyrene and additional solvent. The polystyrene, particle, and solvent solutions homogenize on a roller for an additional 2 days before use.

For neutron scattering experiments, we prepare solutions of nominal 8c^* polystyrene with concentrations of 0, 1, and 10 wt % silica nanoparticles (volume fraction ϕ = 0, 0.004, and 0.042, respectively). Sample compositions are detailed in the Supporting Information, Tables SI and SII. We use both protonated and partially deuterated 2-butanone solvents to vary the contrast between different constituents in the solution (Figure 1). For neutrons, the scattering

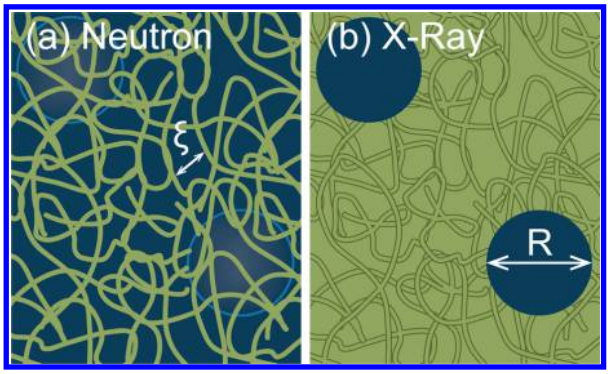

Figure 1. Schematic illustrating the scattering contrasts for silica particles of radius R dispersed in semidilute polystyrene with correlation length ξ for (a) neutrons with partially deuterated solvent and for (b) X-rays.

length densities (SLDs) in 10^{-6} Å^{-2} are calculated to be 1.412 for polystyrene, 3.469 for silica, 0.166 for 2-butanone, and 3.667 for d_5-2-butanone. Samples prepared with the protonated solvent are loaded into 1 mm thick titanium cells with quartz windows to prevent multiple scattering, whereas the samples prepared with the deuterated solvent are loaded into 2 mm thick cells to increase the scattering intensity. We collect small-angle neutron scattering (SANS), ultra-small-angle neutron scattering (USANS), and neutron spin-echo (NSE) data on the NGB30, BT5, and NSE beamlines, respectively, at the Center for Neutron Research, National Institute of Standards and Technology.[32,33] The raw SANS and USANS data are corrected for detector sensitivity, empty cell scattering, and blocked beam scattering and normalized to absolute intensity using IgorPro.[34] The USANS data are desmeared in IgorPro using the slit geometry of the beamline.

DOI: 10.1021/acs.macromol.6b01277
Macromolecules 2016, 49, 6568−6577

The SANS and USANS curves are then merged together without any additional scaling and show excellent agreement in absolute scattering intensity in their overlapping region (Supporting Information, Figure S2). Incoherent scattering intensity is determined by linear fits to $I(Q)$ Q^4 vs Q^4 and subtracted from the absolute scattering to generate coherent scattering curves $I_{coh}(Q) = I_{total}(Q) - I_{incoh}(Q)$ (Supporting Information, Figure S3). The NSE data are corrected for the instrumental resolution and for solvent dynamics by collecting echoes on a charcoal standard and on pure d_8-2-butanone, respectively. The NSE data are reduced using the DAVE software package.[35]

For X-ray scattering experiments, we prepare solutions of nominal 5.5c*, 8c*, and 12.5c* polystyrene and 1, 3, and 10 wt % silica in 2-butanone (ϕ = 0.004, 0.012, and 0.042, respectively). We also run X-ray scattering experiments on the same (deuterated) solutions used for the neutron scattering experiments to ensure the solution structure is unaffected by deuterated solvent. The neutron samples are sealed after the neutron scattering experiments and stored at 0−4 °C for 6 months between the two experiments, much longer than any intrinsic time scale associated with these dispersions, with no aggregation or sedimentation of the particles. The SLDs for X-rays in 10^{-6} Å^{-2} are calculated to be 9.607 for polystyrene, 18.831 for silica, and 7.603 for 2-butanone and d_8-2-butanone. The solutions are loaded into 1 mm i.d. boron-rich quartz capillary tubes (Charles-Supper) and sealed with wax to prevent evaporation. We collect X-ray photon correlation spectroscopy (XPCS) and low-Q small-angle X-ray scattering (SAXS) data over a wavevector range 0.0019 Å^{-1} < Q < 0.012 Å^{-1} at the X-ray photon correlation spectroscopy beamline 8-ID-I at the Advanced Photon Source, Argonne National Laboratory. The temperature is controlled by attaching the samples to a block of copper held at constant temperature using a Peltier plate. Autocorrelation curves are collected at five separate points on the sample and averaged together with error propagated through the fitting procedure. We collect the high-Q SAXS data over a wavevector range 0.007 Å^{-1} < Q < 0.3 Å^{-1} on a Rigaku S-MAX3000 beamline at the University of Houston. The SAXS data are corrected for background scattering. Background scattering is determined in the same fashion as the incoherent neutron data and removed from the total scattering intensity to produce the coherent scattering data. All SAXS, SANS, and USANS data are analyzed using SASView.

Zeta potential of the silica nanoparticles is measured in 2-butanone using a NanoBrook ZetaPALs (Brookhaven Instruments) analyzer and repeated five times to assess experimental error. Particle concentration is kept constant at volume fraction of 7.5 × 10^{-5} in all solutions. Dynamic light scattering (DLS) data are collected with an ALV goniometer equipped with a He−Ne laser (632.8 nm) and an ALV-5000/EPP Multiple tau digital correlator (ALV-GmbH, Langen, Germany). Intensity correlation functions $G_2(Q,\Delta t)$ are collected at 45°, 60°, 75°, 90°, 105°, and 120° and fit to single-exponential functions $G_2(Q,\Delta t) = A + B\exp(-2\Gamma\Delta t)$, where $A \approx 1$ relates to the autocorrelation at long times, $B \approx 1$ represents the autocorrelation of the particles at short times, and Γ is the relaxation rate. The particle diffusivity D is calculated by fitting $\Gamma = DQ^2$. The hydrodynamic radius of the particle is then calculated from the Stokes−Einstein equation $R_H = k_BT/(6\pi\eta D)$, where k_B is the Boltzmann constant and η is the viscosity of the solution as determined from intrinsic viscosity experiments (Supporting Information).

3. RESULTS AND DISCUSSION

3.1. Structure of Particle Dispersion. We use SAXS to investigate the structure of the silica nanoparticles in solution as a function of particle and polymer concentration. In X-rays, the difference between the SLDs for silica and the solvent is much greater than the contrast between the polymer and the solvent and the scattering from the nanoparticles dominates (Figure 1b). For all particle loadings and all polymer concentrations, we observe a strong Q^{-4} scaling at high Q, corresponding to the particle interface, and a clearly defined structure factor at intermediate Q that exhibits a local maximum at Q*. The appearance of a sharp structure factor at relatively low volume fractions of particles indicates that the particles are charged with long-range electrostatic repulsion, as seen previously for silica particles from the same manufacturer in a different organic solvent (dimethylacetamide).[36] We fit the SAXS data to $I(Q) = AS(Q)P(Q)$ where $P(Q)$ represents the spherical form factor[37] given by

$$P(Q) = \left[\frac{\sin(QR) - QR\cos(QR)}{(QR)^3}\right]^2 \quad (1)$$

and $S(Q)$ is the structure factor for charged spheres[38,39] (Figure 2). A is a scaling factor related to the difference in SLDs and the volume of scatterers, and R is the nanoparticle radius. We note that $S(Q)$ depends on the relative permittivity of the solvent ε = 18.5, particle radius R, salt concentration c_{salt} = 0 g/L, temperature T = 298 K, volume fraction of particles ϕ, and charge on the particle surface z_m. We refer the interested reader to the full expression of $S(Q)$ provided in ref 38. The form factor and structure factor are fit simultaneously for all solutions using a global R = 24.0 ± 0.1 nm with a log-normal polydispersity of 0.28 ± 0.02, in close agreement with the manufacturer's specification.[b] For the structure factor, we specify all quantities with the exception of ϕ and z_m that are treated as fitting parameters (Supporting Information Table SIII).

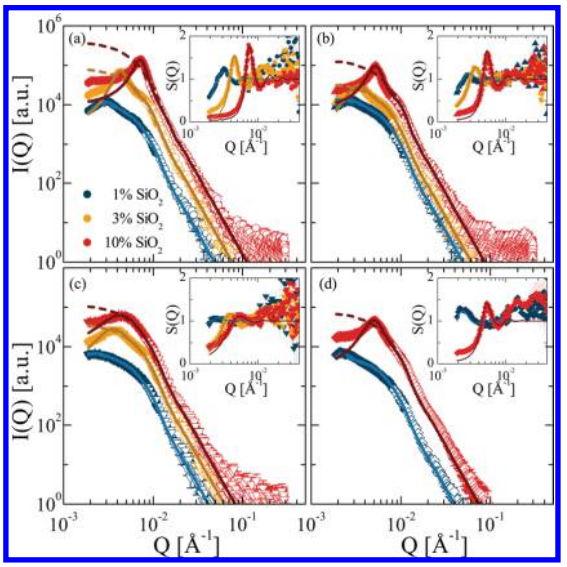

Figure 2. SAXS intensity $I(Q)$ showing the structure of the silica nanoparticles in (a) pure solvent and in solutions of (b) 5.5c*, (c) 8c*, and (d) 12.5c* polystyrene with varying concentrations of silica. Scattering data were collected at Argonne National Lab (closed) and the University of Houston (open). Data shifted to agree in the overlapping Q region. Solid curves represent fits to overall intensity. Dashed curves indicate spherical form factor. Insets: structure factor $S(Q)$ of the same solutions. Solid curves are fits to the Hayter model for charged spheres.

To assess the dispersion of the nanoparticles, we determine the center-to-center interparticle distance $x_{ID} = 2\pi/Q$*. Assuming ideal dispersion of the particles, we estimate the interparticle distance as $x_{ID} \approx 2R/(\phi/\phi_{max})^{1/3}$, where ϕ is the volume fraction of silica particles and ϕ_{max} = 0.64 represents the volume fraction of monodisperse hard spheres at random close packing.[19] The measured interparticle distance agrees very

DOI: 10.1021/acs.macromol.6b01277
Macromolecules 2016, 49, 6568−6577

closely with the estimated interparticle distance for all polystyrene and silica concentrations (Table 1).

Table 1. Estimated and Measured Interparticle Distance x_{ID} for Various Solutions as a Function of Polystyrene and Silica Loadings

		x_{ID} from $S(Q)$ [nm ± 5]			
silica (wt %)	est x_{ID} [nm]	0c^* PS	5.5c^* PS	8c^* PS	12.5c^* PS
1	240	200	210	240[a]	270
3	170	140	170	160	N/A
10	110	85	120	120[a]	120

[a]Solutions of d_5-2-butanone were used for neutron scattering experiments.

The dispersion of the particles is maintained by the electrostatic repulsions between particles in the organic solvent. Using the parameters extracted from the SAXS fits, we calculate the zeta potential $\zeta = z_m \exp(-\kappa R)/4\pi\varepsilon_0\varepsilon$, where ε_0 is permittivity of a vacuum, $\kappa = (z_m^2 n_m/\varepsilon_0\varepsilon k_B T)^{1/2}$ is the inverse of the Debye length, and n_m is the particle number density. We also directly measure ζ in dilute particle dispersions in the presence of small amounts of polymer. We are unable to directly measure the ζ potential at higher particle and polymer concentrations because of multiple scattering effects and high solution viscosity, respectively. The measured and calculated ζ potentials agree within experimental error for all polymer concentrations (Figure 3); the polystyrene does not screen the

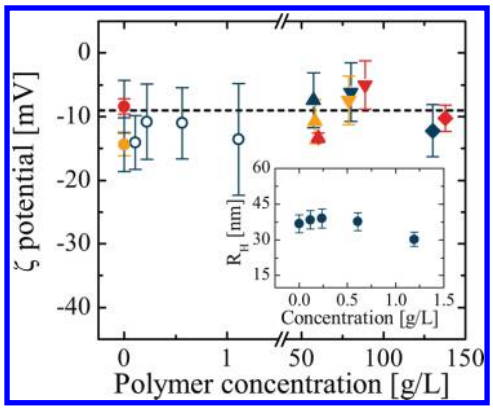

Figure 3. Zeta potential of silica nanoparticles as a function of polymer concentration. Open symbols indicate dilute particle dispersions. Closed symbols calculated from SAXS with same symbols as in Figure 2. Blue, yellow, and red symbols correspond to silica loadings of 1, 3, and 10 wt %. Dashed line is average of closed symbols. Inset: hydrodynamic nanoparticle radius R_H from DLS measurements as a function of polymer concentration.

charge between the particles. Additionally, we find no substantial change in the nanoparticle hydrodynamic radius as a function of polymer concentration (inset to Figure 3), indicating that the polymer does not adsorb to the surface of the particles. Thus, the interactions between particles and polymer are neutral or, more likely, weakly repulsive whereas the particle−particle interaction is strongly repulsive. Although the particles are well-dispersed in solution up to 12.5c^* PS, significant particle aggregation when $c/c^* > 15$ arises from the increase in the depletion attraction between the silica particles from $-40k_BT$ to $-100k_BT$ for 5.5c^* and 16c^* solutions, respectively (Supporting Information, Figures S4 and S5).[40−44]

Because of particle aggregation, we do not report dynamics in solutions with $c/c^* > 15$ in this work. Additionally at low Q, the SAXS fits consistently underestimate the measured intensity at high silica concentrations, suggesting that structures may exist on even larger length scales.

We use small-angle and ultrasmall-angle neutron scattering to investigate the nanoparticle structure on larger length scales ranging up to micrometers. In protonated solvent, the scattering intensity of the silica nanoparticles dominates with small contributions from the polymer chains at high Q (Figure 4a). The scattering data for the 8c^* PS 10% SiO_2 solution closely agrees with that measured using SAXS in the overlapping Q range, but at lower Q values inaccessible on the SAXS beamlines, the scattering intensity exhibits a large upturn indicative of large scale fractal structures. We model the scattering intensity from SANS and USANS in protonated solvent as the sum of a Lorentzian term describing the correlation length between polymer chains and spherical and mass fractal[45] contributions describing the particle structure according to

$$I_{coh}(Q) = \frac{A}{1 + (Q\xi)^2} + [BS_s(Q) + CS_{MF}(Q)]P(Q) \quad (2)$$

where $P(Q)$ is the spherical form factor given in eq 1, $S_{MF}(Q)$ is the mass fractal structure factor given by

$$S_{MF}(Q) = \frac{\Gamma(D_m - 1)\xi_{MF}^{D_m - 1}}{[1 + (Q\xi_{MF})^2]^{(D_m - 1)/2}} \frac{\sin[(D_m - 1)\tan^{-1}(Q\xi_{MF})]}{Q} \quad (3)$$

and $S_s(Q)$ is the structure factor for charged spheres. In these expressions, A, B, and C are scaling constants relating to the scattering intensity from polymer chains, individual particles, and the mass fractal, respectively, ξ is the polymer correlation length, D_m is the fractal dimension, $\Gamma(x)$ is the gamma function, and ξ_{MF} is the fractal correlation length that relates to the overall fractal radius $R_{MF} = (D_m(D_m + 1)\xi_{MF}^2/2)^{1/2}$.[46]

In the range $\xi_{MF}^{-1} \leq Q \leq R^{-1}$, $S_{MF}(Q)P(Q)$ scales as Q^{-D_m}.[45] Fixing the particle radius R = 24 nm with a log-normal polydispersity of 0.28 as measured in SAXS and the polymer correlation length ξ = 3.9 nm according to the fits on partially deuterated solvents (section 3.2), we fit the structure and form factors simultaneously to extract D_m, ξ_{MF}, interparticle distance $x_{ID} = 2\pi/Q^*$, and particle charge z_m. The scattering from the polymer chains dominates when $Q > 0.1$ Å^{-1}. When 0.005 Å^{-1} < Q < 0.1 Å^{-1}, the scattering data follow the form and structure factor for individual particles with an interparticle distance of 124 ± 5 nm, which is in very close agreement with the measured interparticle distance from SAXS.

At very small wavevectors $Q < 0.001$ Å^{-1}, the upturn in scattering intensity indicates that silica nanoparticles arrange in mass fractals with a fractal dimension $D_m = 2.29 \pm 0.05$, similar to that seen for reaction-limited aggregates,[47] reversible clusters,[48] and composites containing well-dispersed nanoparticles[49] and nanorods.[50] The agreement between SAXS and (U)SANS over a 6 month period suggests that the fractal structures are formed from reversible long-range interactions. Additionally, the agreement between Q^* and estimates for x_{ID} indicates that the majority of the particles are surrounded by the polymer solution rather than in direct contact with other particles, even within the fractal clusters. We conclude that individual particles are well dispersed within the semidilute polymer solutions with a center-to-center interparticle distance

DOI: 10.1021/acs.macromol.6b01277
Macromolecules 2016, 49, 6568−6577

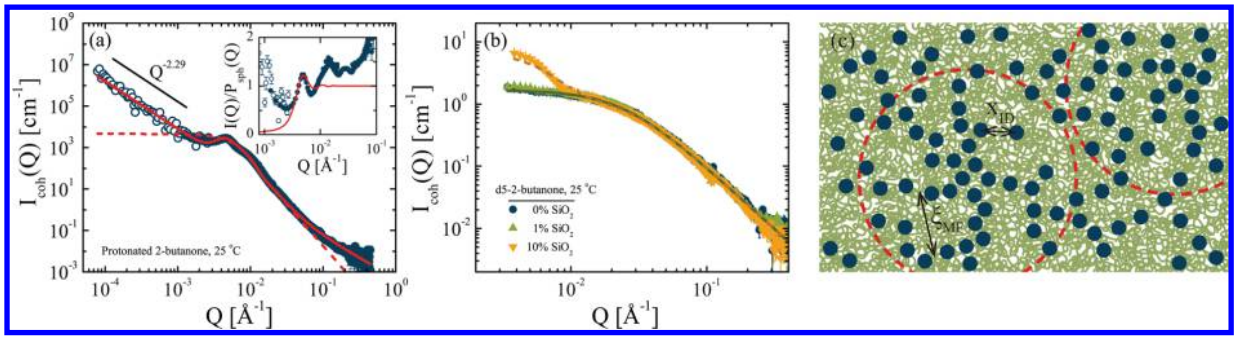

Figure 4. (a) Coherent scattering intensity $I_{coh}(Q)$ from USANS (○) and SANS (●) showing the structure of silica particles in the 8c* PS 10% SiO_2 solution in protonated 2-butanone at 25 °C. Solid curve is overall fitted intensity from eq 2. Dashed curve is the spherical form factor fit. Absence of a low-Q plateau in the USANS data indicates that $\xi_{MF} > 1$ μm. Inset: overall intensity divided by the spherical form factor. Solid curve is fit to the Hayter model for charged spheres.[38] (b) Coherent SANS scattering intensity $I_{coh}(Q)$ showing the structure of the polymer in 8c* PS solutions and various concentrations of silica particles in d_5-2-butanone at 25 °C. Solid curves are fits to Lorentz form factors (eq 4). Dashed curve is fit to sum of Lorentz and spherical form factors (eqs 1 and 4). (c) Schematic of structure for a particle dispersion in a semidilute polymer solution with interparticle distance x_{ID} and fractal correlation length ξ_{MF}. Dashed curves encircle fractal centers with radius $R_{MF} > 10$ μm. Relevant length scales labeled but not drawn to scale.

x_{ID} and form fractal clusters on larger length scales, shown schematically in Figure 4c. Because the nanoparticles and polymer are comparably sized ($R \sim R_{g,0}$), the dynamics of the particles depends on the structure and relaxation modes of the polymer chains.[14,18] Thus, we must first characterize the polymer structure and dynamics in the presence of particles before analyzing the particle dynamics.

3.2. Structure of Polymer Chains. Switching solvents to d_5-2-butanone increases the contrast between the polymer and the solvent (SLD difference $\Delta\rho = 2.255 \times 10^{-6}$ Å^{-2}) and decreases the contrast between the solvent and particles ($\Delta\rho = 0.198 \times 10^{-6}$ Å^{-2}). The resulting scattering data allow us to precisely characterize the polymer structure in the presence of particles (Figure 1a). The coherent scattering data are well fit by a Lorentz form factor for Gaussian coils in semidilute solutions

$$I_{coh}(Q) = \frac{I_0}{1 + (Q\xi)^2} \tag{4}$$

where I_0 is the scattering intensity at $Q = 0$ (Figure 4b). At a silica loading of 10 wt %, there is some signal from the nanoparticles at low Q due to imperfect contrast matching; the full scattering data are then well fit to the sum of Lorentz and spherical form factors (Supporting Information, Figure S6). Polymer scaling laws predict that $\xi \approx R_{g,0}(c/c^*)^{-\nu/(3\nu-1)}$, where $\nu = 0.53$ is the inverse of the fractal dimension for polystyrene in 2-butanone.[29,30,51] For the 8c* PS solution in the absence of particles, we find $\xi = 4.1 \pm 0.1$ nm, in good agreement with the prediction from scaling theory of $\xi \approx 4.3$ nm.

To determine the effect of the particles on the polymer structure, we measure the scattering pattern as a function of particle loading. For a silica loading of 1 wt %, the measured correlation length $\xi = 4.1 \pm 0.1$ nm agrees with that measured in the absence of particles. For a silica loading of 10 wt %, however, we find $\xi = 3.9 \pm 0.1$ nm. Because an entropic penalty prevents polymer chains from residing near a particle surface,[52] we expect a depletion layer with a thickness on the order of ξ to surround each particle.[53] For fully dispersed particles, the total excluded volume of the system is $\phi_{ex} = \phi_{NP}[(R_{NP} + \xi)/R_{NP}]^3$, where ϕ_{NP} is the nanoparticle volume fraction. In a solution of 1 wt % silica, $\phi_{ex} = 0.008$ does not significantly alter the effective polystyrene concentration; for a silica loading of 10 wt %, $\phi_{ex} = 0.072$ becomes significant. To incorporate excluded volume into the scaling theory, we calculate the concentration of polymer in the free volume as $c_{free} = c/(1 - \phi_{ex})$. At a particle loading of 10 wt %, scaling theory predicts $\xi \approx 3.9$ nm using c_{free}, which agrees with the value measured from SANS. Thus, the particles induce slight changes in the polymer correlation length by introducing excluded volume but do not change the overall Gaussian conformation of the chains.

3.3. Polymer Dynamics Investigated Using NSE. Specific particle−polymer interactions can significantly change the relaxation modes of a polymer chain near a particle surface.[54−58] To assess potential changes in the polymer dynamics, we conduct NSE experiments on the same d_5-2-butanone samples used for SANS. We first measure the polymer dynamics in the absence of particles over a wide range of wavevectors 0.015 Å^{-1} < Q < 0.1 Å^{-1}, corresponding to $0.65 \leq Q\xi \leq 4.3$, and over a wide time range from 0.1 to 150 ns. The normalized intermediate scattering functions decay according to a stretched exponential as $S(Q,t)/S(Q,0) = A \exp(-(\Gamma t)^{\beta})$, where $A \approx 1$ for fully correlated dynamics on short time scales and β is the stretching exponent. The polymer dynamics follows the Zimm model with $\beta = 2/3$ as predicted when $Q\xi \gtrsim 1$.[59] In the Zimm model, the relaxation rate Γ depends only on solvent viscosity η_0 and wavevector Q according to $\Gamma = (k_B T/6\pi\eta_0)Q^3$ (Figure 5).[60] The collapse of the autocorrelation curves onto a single master curve, albeit with a viscosity $\eta \approx 2\eta_0$, indicates that the polymer repeat units are hydrodynamically coupled over the length and time scales investigated. Over larger distances when $Q \ll \xi^{-1}$, we expect the hydrodynamic coupling to decay so that the polymer moves as a Rouse chain of hydrodynamic blobs with a size comparable to ξ.[30]

To determine the effect of nanoparticles on polymer dynamics, we measure dynamics as a function of particle loading. The autocorrelation curves for different particle concentrations obey the same Zimm scaling, as evidenced by a collapse onto a single curve as a function of $(Q^3t)^{2/3}$ (Figure 6). The polymer dynamics follow the Zimm model in these solutions because we probe length scales within a correlation blob $Q\xi \gtrsim 1$ and short time scales.[61] In contrast to the hydrodynamic coupling between polymer repeat units, the lack of change in polymer dynamics as a function of particle loading indicates that the polymer is not hydrodynamically coupled to the particle over the length and time scales investigated here.

DOI: 10.1021/acs.macromol.6b01277
Macromolecules 2016, 49, 6568−6577

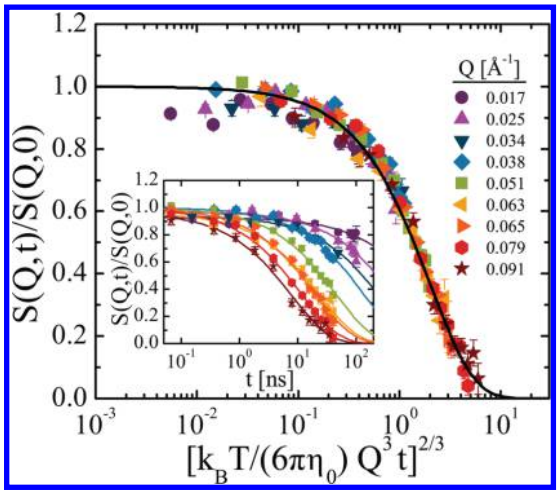

Figure 5. Normalized dynamic correlation function $S(Q,t)/S(Q,0)$ as a function of Zimm scaling for polymer dynamics in a solution of 8c* polystyrene and d_5-2-butanone at 25 °C. Solid curve represents a single-exponential fit with a viscosity $\eta = 2\eta_0$. Inset: individual correlation curves as a function of lag time t. Curves are fits to a stretched exponential with $\beta = 2/3$.

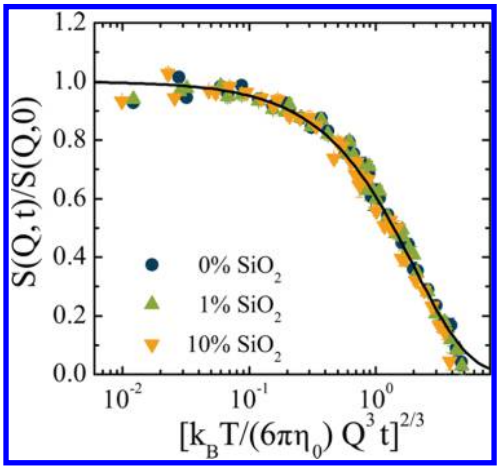

Figure 6. Normalized dynamic correlation function $S(Q,t)/S(Q,0)$ as a function of Zimm scaling for polymer dynamics in nominal 8c* PS solutions of varying silica concentration in d_5-2-butanone at 25 °C. Solid curve is single-exponential fit with $\eta = 2\eta_0$. Only data for Q = 0.025, 0.051, and 0.079 Å^{-1} are shown for clarity.

Physically, there may be two possible explanations for the lack of a measurable change in the polymer dynamics. First, because hydrodynamic interactions are screened over ξ in semidilute solutions, only a fraction of polymer ($\lesssim$10%) may be hydrodynamically affected by the particle. Second, internal polymer relaxations are only modestly affected by the particle surface when the particle−polymer interactions are neutral or weakly repulsive,[62,63] as investigated here. By contrast, for systems with highly attractive particle−polymer interactions, small particle loadings significantly change the polymer dynamics.[57] Thus, the lack of a measurable change in the polymer dynamics suggests that the polymer is not affected by the particles. Because the relaxation time of the polymer at fixed Q does not vary across particle concentration, the subdiffusive particle dynamics caused by coupling to the polymer is expected to remain constant with increasing particle concentration.

3.4. Particle Dynamics Investigated Using XPCS. We run XPCS experiments on solutions of varying silica and polymer concentrations to measure the dynamics of interacting nanoparticles in semidilute polymer solutions. We measure the intensity autocorrelation curves G_2 for the nanoparticles over a wide range of wavevectors 0.002 Å^{-1} < Q < 0.011 Å^{-1} corresponding to 0.45 < QR < 26 and on time scales Δt > 1 ms. We first fit the intensity autocorrelation curves G_2 using a double-exponential decay, but we see systematic oscillatory deviations in the residuals (Supporting Information, Figure S8). Instead, the curves are well fit by a stretched exponential according to $G_2(Q,\Delta t) = 1 + BG_1(Q,\Delta t)^2 + \varepsilon$, where B is the Siegert factor that depends on the experimental geometry, $G_1(Q,\Delta t) = \exp(-(\Gamma\Delta t)^\beta)$ is the field correlation function, β is a stretching exponent, and ε captures any residual noise. B and ε depend on the experimental design and geometry and are thus Q-independent. We find that β does not vary significantly with Q for our samples (Supporting Information, Figure S7) and therefore fit the correlation curves using global values of B, β, and ε for each solution (Figure 7a).

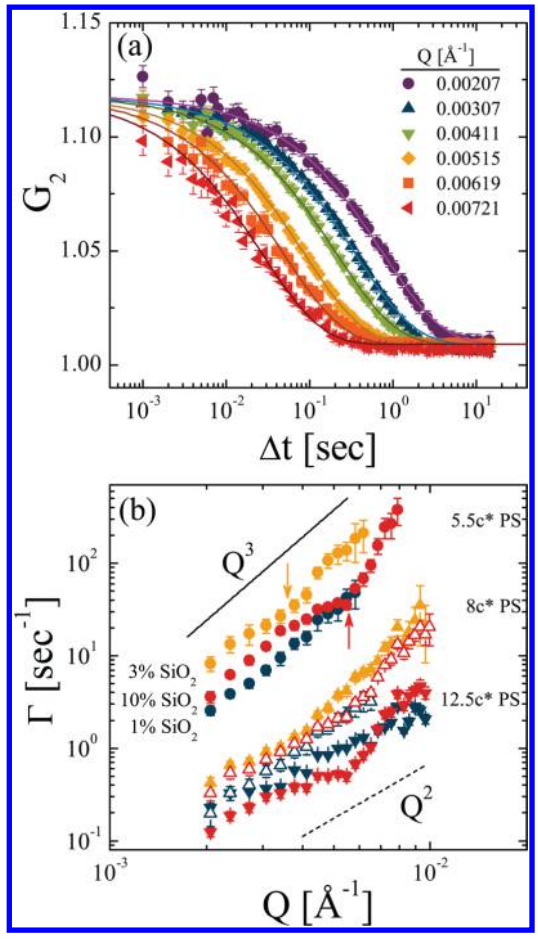

Figure 7. (a) Representative intensity autocorrelation functions G_2 for particle dynamics as a function of lag time Δt at various wavevectors Q for the 8c* PS 3% SiO_2 solution. Solid curves are stretched exponential fits with β = 0.60. (b) Relaxation rate Γ of particle dynamics as a function of wavevector Q for solutions of nominal 5.5c* (○), 8c* (△), and 12.5c* (▽) polystyrene and silica concentrations of 1 (blue), 3 (yellow), and 10 wt % (red). Open symbols represent the solutions used in neutron scattering experiments. Solid and dashed lines indicate Q^3 and Q^2 scaling, respectively. Arrows indicate deviations from Q^3 scaling for the 5.5c* PS solutions.

DOI: 10.1021/acs.macromol.6b01277
Macromolecules 2016, 49, 6568−6577

From the stretched exponential fits, we extract the corresponding relaxation rate Γ as a function of Q (Figure 7b). The relaxation rates steadily decrease with increasing polymer concentration as expected because the additional polymer leads to a higher bulk viscosity. With increasing silica concentration, however, the relaxation rates do not vary monotonically or consistently across polymer concentrations and the variations are much smaller than the change in dynamics with increasing polymer concentration. We expect the particle dynamics to be similar across different silica concentrations because the particles remain well dispersed, the polymer coils remain Gaussian, and the polymer dynamics does not change with silica concentration. The similar dynamics in solutions of similar polymer concentrations indicate that the individual particles indeed experience the same local environment regardless of silica concentration.

At all polymer and silica concentrations, we notice an unexpected scaling of the relaxation rates with Q. We find $\Gamma \sim Q^3$ rather than the classical scaling $\Gamma \sim Q^2$ for diffusive motion (Figure 7b). For colloidal motion through a polymer solution in which $\xi < R$, particle motion is coupled to the dynamics of the polymer; this coupling leads to subdiffusion on short time scales, so that the mean-squared displacement of the particle $\langle \Delta r^2 \rangle \sim \Delta t^{\beta}$ with $\beta \leq 1$.[14,18,64] Physically, the intermediate scattering function relates to the particle displacement through $G_1(Q,\Delta t) = \exp(-\langle \Delta r^2 \rangle Q^2/6)$. Substitution of subdiffusive dynamics gives $G_1(Q,\Delta t) \approx \exp(-(Q^{2/\beta}\Delta t)^{\beta})$. Thus, the stretched exponential decays indicate subdiffusive particle dynamics only if $\Gamma \sim Q^{2/\beta}$, as suggested in ref 65. Indeed, we measure $\beta \approx 2/3$ and $\Gamma \sim Q^3$ (Table 2 and Figure 7b) and verify that the Q-scaling and β are independent of each other (Figure S9).

Table 2. Stretching Exponent β from Stretched Exponential Fits to XPCS Data for Solutions of Various Silica and Polystyrene Concentrations

	stretching exponent $\beta \pm 0.02$		
silica (wt %)	5.5c* PS	8c* PS	12.5c* PS
1	0.56	0.62[a]	0.71
3	0.56	0.60	
10	0.59	0.56[a]	0.66

[a]Solutions of d_5-2-butanone were used for neutron scattering experiments.

Although our data are consistent with subdiffusive particle dynamics, the stretching exponent is larger than the theoretically predicted[14] and experimentally measured[65] exponent $\beta = 0.5$ for particle motion in concentrated polymer solutions when $R > \xi$. Whereas the previous experimental work[65] used particles that were larger than the tube diameter, here we investigate particle dynamics in less concentrated solutions in which the tube diameter ranges from 35 nm at 12.5c* PS to 75 nm at 5.5c* using $a(\phi) = a(1)\phi^{-0.76}$ in a good solvent, where $a(1) \approx 8$ nm is the tube diameter in a polystyrene melt.[30,66] Thus, the tube diameter is comparable to or larger than the particle radius in all of our solutions, and we do not see entanglement-controlled behavior. Instead, our stretching exponents $\beta \approx 2/3$ agree well with our previous work measuring particle displacements in semidilute, unentangled solutions when $R/R_{g,0} \approx 1$.[18]

The coupling between particle and polymer dynamics derives from relaxations over ξ, but over the interparticle distance there are significant deviations from the overall Q^3 scaling (arrows in Figure 7b). For example, the dynamics is suppressed in the 5.5c* PS 10% SiO_2 sample around $Q = 0.0055$ Å^{-1}, near the local maximum in $S(Q)$. This suppression is reminiscent of de Gennes narrowing seen in hard colloidal[23,67−70] and multiarm polymer[71,72] systems. In colloidal dispersions, the dynamics and structure are inversely related through $D(Q) = D_0H(Q)/S(Q)$, where $H(Q)$ represents hydrodynamic effects and D_0 is the diffusivity of the particle in the absence of hydrodynamics and structure. Although hydrodynamics is screened over ξ in polymer solutions[59] so that $H(Q\xi < 1) = 1$, the sharp peaks in $S(Q)$ (Figure 2) suggest that structural effects are important. In our system, however, a diffusion constant is not well-defined because the particles move subdiffusively on all accessible time scales. Instead, we define an analogous kinetic parameter K that satisfies $\Gamma = KQ^3$. Over long length scales, the particle dynamics should be coupled to the particle structure according to the de Gennes narrowing predictions. Therefore, we compare the normalized kinetic parameter $K_0/K(Q)$ as a function of Q to the $S(Q)$ fits for each solution (Figure 8). K_0 represents the particle dynamics in the absence of structural relaxations and is determined from the relaxation rate when $S(Q)$ is first equal to 1 after the structural peak.

In the absence of any fitting parameters, the peak position and shape of $K_0/K(Q)$ are captured by $S(Q)$ for all polymer and particle loadings that exhibit stretched exponential relaxations with $\beta \approx 2/3$. The close agreement between structure and dynamics indicates that the particle dynamics depends strongly on interparticle interactions despite the coupling to polymer dynamics over short time and length scales. Although the polymer mesh presents an energy barrier to particle motion that leads to the coupling between particle and polymer dynamics,[14] the particles cannot be entirely trapped by the correlation mesh or the particles would no longer interact over longer length scales. For example, the de Gennes narrowing of particle dynamics disappears in glassy fluids as the liquid approaches the glass transition temperature T_g[73] because of effectively infinite energy barriers between particles in different cooperatively rearranging regions.[74,75] By contrast, the polymer correlation mesh in semidilute solutions must introduce only a finite energy barrier to particle motion, with the interparticle interactions providing an additional energy barrier.

Our independent measurements of the dynamics of both particles and polymer demonstrate the coupling between the two components, even though the experimental methods access widely separated length and time scales. Specifically, XPCS investigates length scales 1 order of magnitude larger than and time scales 4 orders of magnitude longer than those probed by NSE. Given these differences in length and time scales, the subdiffusive dynamics that we measure for polymer relaxations is not physically the same as that measured for the particles. Bridging these time and length scales, while experimentally challenging, will shed light onto the physical origins of the coupling and hence relate the local movements of particles to the mobility of polymer chains.

4. CONCLUSION

We study the dynamics of nanoparticles in semidilute solutions in which the particle and polymer are comparably sized and in which interparticle interactions are present. We tune the

DOI: 10.1021/acs.macromol.6b01277
Macromolecules 2016, 49, 6568−6577

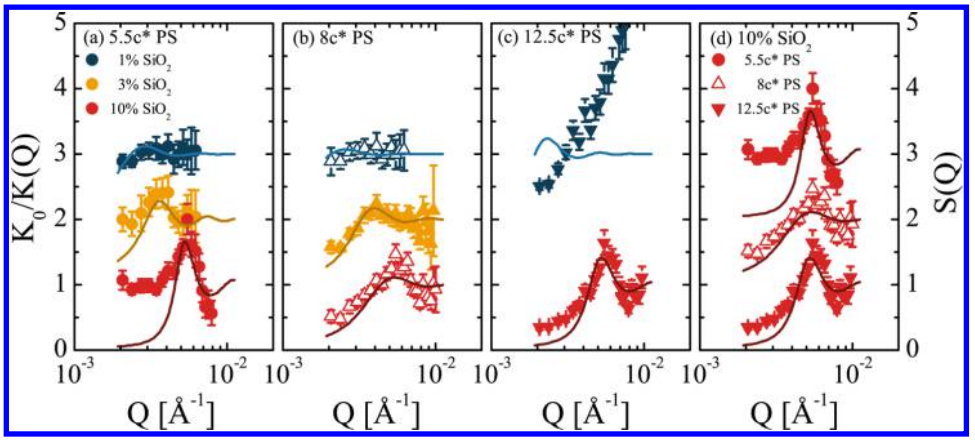

Figure 8. Normalized dynamic factor $K_0/K(Q)$ for silica dynamics as a function of wavevector Q for solutions of nominal (a) 5.5c* (○), (b) 8c* (△), and (c) 12.5c* (▽) polystyrene concentrations for different silica concentrations and (d) 10 wt % silica for various polymer concentrations. Solid lines represent structure factor $S(Q)$ of corresponding solution. Data and structure factors shifted vertically by unit increments for clarity with actual high Q plateaus at $S(Q) = 1$. Open symbols represent samples used in neutron scattering. Deviation in the 12.5c* PS 1% SiO_2 solution arises because $\beta > 2/3$ for this sample so that $Q^{2/\beta} \neq Q^3$.

scattering contrast within the solutions to measure the structure and dynamics of the polymer chains with neutrons and those of the particles with X-rays. In the presence of polystyrene, the silica nanoparticles remain stable and well dispersed. Structurally, the polymer coils adopt a Gaussian configuration with a correlation length that decreases slightly with increasing particle loading due to the increase in excluded volume. The polymer dynamics agrees with the Zimm model regardless of particle concentration, indicating that the particle−polymer coupling is unchanged at higher particle loadings. The nanoparticle dynamics is subdiffusive in the polymer solutions and exhibits de Gennes narrowing at the particle structure factor peak. Our results suggest that particle dynamics cannot be fully described through coupling to the relaxations of the semidilute polymer mesh on short length scales but must also include contributions from the interparticle interactions over longer distances.

This model system is a potential framework from which to investigate a variety of parameters that affect the structure and dynamics in complex fluids and nanocomposite materials. For example, chemical and electrostatic interactions between the particle and polymer can be controlled by chemically modifying the particle surface, functionalizing the polymer, or changing the salt concentration. Physical interactions can be added by grafting onto the particle surface polymer that is either chemically similar[76] or dissimilar[77] to the free polymer. The ability to selectively characterize the dynamics and structure of specific components in a multicomponent system will lead to significantly improved control over the properties of new composite materials and the transport properties of particles through complex environments, such as biological tissue[78] or porous media.[79,80]

■ ASSOCIATED CONTENT

Supporting Information

The Supporting Information is available free of charge on the ACS Publications website at DOI: 10.1021/acs.macromol.6b01277.

Intrinsic viscosity and dynamic light scattering measurements, detailed sample concentrations, detailed analysis of SANS and USANS data, calculation of incoherent and background scattering, analysis of aggregation in concentrated polystyrene solutions, estimates of interparticle potentials, and details on XPCS curve fitting. (PDF)

■ AUTHOR INFORMATION

Corresponding Authors

*E-mail: jcconrad@uh.edu (J.C.C.).
*E-mail: ramanan@uh.edu (R.K.).

Notes

The authors declare no competing financial interest.

■ ACKNOWLEDGMENTS

We thank Drs. Peter Vekilov at the University of Houston and Michael Wong at Rice University for access to the DLS and zeta potential instruments, respectively. This work utilized the NIST Center for Neutron Research (NCNR) supported in part by the National Science Foundation (NSF) under Agreement DMR-1508249. This research used resources of the Advanced Photon Source, a U.S. Department of Energy (DOE) Office of Science User Facility operated for the DOE Office of Science by Argonne National Laboratory under Contract DE-AC02-06CH11357. This work benefited from SasView software, originally developed by the DANSE project under NSF Award DMR-0520547. The SAXS experiments at UH were performed on an instrument obtained on an NSF grant (NSF DMR 1040446). R.K. and R.P.S. acknowledge funding from ExxonMobil Company. J.C.C. acknowledges funding from NSF (CBET-1438204) and the Welch Foundation (E-1869).

■ ADDITIONAL NOTES

[a]The identification of any commercial product or trade name does not imply endorsement or recommendation by the National Institute of Standards and Technology.
[b]Throughout this article, error bars and uncertainties represent one standard deviation.

■ REFERENCES

(1) Sandler, J.; Shaffer, M.; Prasse, T.; Bauhofer, W.; Schulte, K.; Windle, A. H. Development of a dispersion process for carbon nanotubes in an epoxy matrix and the resulting electrical properties. *Polymer* **1999**, *40*, 5967−5971.

DOI: 10.1021/acs.macromol.6b01277
Macromolecules 2016, 49, 6568−6577

(2) Liu, W.; Liu, N.; Sun, J.; Hsu, P.-C.; Li, Y.; Lee, H.-W.; Cui, Y. Ionic Conductivity Enhancement of Polymer Electrolytes with Ceramic Nanowire Fillers. *Nano Lett.* **2015**, *15*, 2740−2745.
(3) Bockstaller, M. R.; Thomas, E. L. Optical Properties of Polymer-Based Photonic Nanocomposite Materials. *J. Phys. Chem. B* **2003**, *107*, 10017−10024.
(4) Sanchez, C.; Lebeau, B.; Chaput, F.; Boilot, J.-P. Optical Properties of Functional Hybrid Organic-Inorganic Nanocomposites. *Adv. Mater.* **2003**, *15*, 1969−1994.
(5) Rafiee, M. A.; Rafiee, J.; Wang, Z.; Song, H.; Yu, Z.-Z.; Koratkar, N. Enhanced Mechanical Properties of Nanocomposites at Low Graphene Content. *ACS Nano* **2009**, *3*, 3884−3890.
(6) Chen, Q.; Gong, S.; Moll, J.; Zhao, D.; Kumar, S. K.; Colby, R. H. Mechanical Reinforcement of Polymer Nanocomposites from Percolation of a Nanoparticle Network. *ACS Macro Lett.* **2015**, *4*, 398−402.
(7) Kalwarczyk, T.; Tabaka, M.; Holyst, R. Biologistics - Diffusion coefficients for complete proteome of Escherichia coli. *Bioinformatics* **2012**, *28*, 2971−2978.
(8) Tang, L.; et al. Investigating the optimal size of anticancer nanomedicine. *Proc. Natl. Acad. Sci. U. S. A.* **2014**, *111*, 15344−15349.
(9) Johnson, E.; Berk, D.; Jain, R.; Deen, W. Hindered diffusion in agarose gels: test of effective medium model. *Biophys. J.* **1996**, *70*, 1017−1023.
(10) Xie, J.; Doroshenko, M.; Jonas, U.; Butt, H.-J.; Koynov, K. Temperature-Controlled Diffusion in PNIPAM-Modified Silica Inverse Opals. *ACS Macro Lett.* **2016**, *5*, 190−194.
(11) Squires, T. M.; Mason, T. G. Fluid Mechanics of Microrheology. *Annu. Rev. Fluid Mech.* **2010**, *42*, 413−438.
(12) Tuteja, A.; Mackay, M. E.; Narayanan, S.; Asokan, S.; Wong, M. S. Breakdown of the Continuum Stokes-Einstein Relation for Nanoparticle Diffusion. *Nano Lett.* **2007**, *7*, 1276−1281.
(13) Wong, I.; Gardel, M.; Reichman, D.; Weeks, E.; Valentine, M.; Bausch, A.; Weitz, D. Anomalous Diffusion Probes Microstructure Dynamics of Entangled F-Actin Networks. *Phys. Rev. Lett.* **2004**, *92*, 178101.
(14) Cai, L.-H.; Panyukov, S.; Rubinstein, M. Mobility of Nonsticky Nanoparticles in Polymer Liquids. *Macromolecules* **2011**, *44*, 7853−7863.
(15) Ye, X.; Tong, P.; Fetters, L. J. Transport of Probe Particles in Semidilute Polymer Solutions. *Macromolecules* **1998**, *31*, 5785−5793.
(16) Cheng, Y.; Prud'homme, R. K.; Thomas, J. L. Diffusion of Mesoscopic Probes in Aqueous Polymer Solutions Measured by Fluorescence Recovery after Photobleaching. *Macromolecules* **2002**, *35*, 8111−8121.
(17) Kalathi, J. T.; Yamamoto, U.; Schweizer, K. S.; Grest, G. S.; Kumar, S. K. Nanoparticle Diffusion in Polymer Nanocomposites. *Phys. Rev. Lett.* **2014**, *112*, 108301.
(18) Poling-Skutvik, R.; Krishnamoorti, R.; Conrad, J. C. Size-Dependent Dynamics of Nanoparticles in Unentangled Polyelectrolyte Solutions. *ACS Macro Lett.* **2015**, *4*, 1169−1173.
(19) Gam, S.; Meth, J. S.; Zane, S. G.; Chi, C.; Wood, B. A.; Winey, K. I.; Clarke, N.; Composto, R. J. Polymer diffusion in a polymer nanocomposite: effect of nanoparticle size and polydispersity. *Soft Matter* **2012**, *8*, 6512−6520.
(20) Ando, T.; Skolnick, J. Crowding and hydrodynamic interactions likely dominate in vivo macromolecular motion. *Proc. Natl. Acad. Sci. U. S. A.* **2010**, *107*, 18457−18462.
(21) De Gennes, P. Liquid dynamics and inelastic scattering of neutrons. *Physica* **1959**, *25*, 825−839.
(22) Hong, L.; Smolin, N.; Smith, J. C. de Gennes Narrowing Describes the Relative Motion of Protein Domains. *Phys. Rev. Lett.* **2014**, *112*, 158102.
(23) Holmqvist, P.; Nägele, G. Long-Time dynamics of concentrated charge-stabilized colloids. *Phys. Rev. Lett.* **2010**, *104*, 058301.
(24) Lurio, L. B.; Lumma, D.; Sandy, A. R.; Borthwick, M. A.; Falus, P.; Mochrie, S. G. J.; Pelletier, J. F.; Sutton, M.; Regan, L.; Malik, A.; Stephenson, G. B. Absence of Scaling for the Intermediate Scattering Function of a Hard-Sphere Suspension: Static and Dynamic X-Ray Scattering from Concentrated Polystyrene Latex Spheres. *Phys. Rev. Lett.* **2000**, *84*, 785−788.
(25) Manley, S.; Wyss, H. M.; Miyazaki, K.; Conrad, J. C.; Trappe, V.; Kaufman, L. J.; Reichman, D. R.; Weitz, D. A. Glasslike Arrest in Spinodal Decomposition as a Route to Colloidal Gelation. *Phys. Rev. Lett.* **2005**, *95*, 238302.
(26) Sigel, R.; Pispas, S.; Vlassopoulos, D.; Hadjichristidis, N.; Fytas, G. Structural Relaxation of Dense Suspensions of Soft Giant Micelles. *Phys. Rev. Lett.* **1999**, *83*, 4666−4669.
(27) Leheny, R. L. XPCS: Nanoscale motion and rheology. *Curr. Opin. Colloid Interface Sci.* **2012**, *17*, 3−12.
(28) Hoffmann, I. Neutrons for the study of dynamics in soft matter systems. *Colloid Polym. Sci.* **2014**, *292*, 2053−2069.
(29) Wagner, H. L. The Mark-Houwink-Sakurada Equation for the Viscosity of Atactic Polystyrene. *J. Phys. Chem. Ref. Data* **1985**, *14*, 1101−1106.
(30) Rubinstein, M.; Colby, R. H. *Polymer Physics*; Oxford University Press: New York, 2003.
(31) Lewis, M. E.; Nan, S. Y.; Yunan, W.; Li, J. B.; Mays, J. W.; Hadjichristidis, N. Analysis of Solution Properties of Polystyrene in 2-Butanone in the Framework of the Hard-Sphere Model. *Macromolecules* **1991**, *24*, 6686−6689.
(32) Glinka, C. J.; Barker, J. G.; Hammouda, B.; Krueger, S.; Moyer, J. J.; Orts, W. J. The 30 m Small-Angle Neutron Scattering Instruments at the National Institute of Standards and Technology. *J. Appl. Crystallogr.* **1998**, *31*, 430−445.
(33) Barker, J. G.; Glinka, C. J.; Moyer, J. J.; Kim, M. H.; Drews, A. R.; Agamalian, M. Design and performance of a thermal-neutron double-crystal diffractometer for USANS at NIST. *J. Appl. Crystallogr.* **2005**, *38*, 1004−1011.
(34) Kline, S. R. Reduction and analysis of SANS and USANS data using IGOR Pro. *J. Appl. Crystallogr.* **2006**, *39*, 895−900.
(35) Azuah, R. T.; Kneller, L. R.; Qiu, Y.; Tregenna-Piggott, P. L. W.; Brown, C. M.; Copley, J. R. D.; Dimeo, R. M. DAVE: A Comprehensive Software Suite for the Reduction, Visualization, and Analysis of Low Energy Neutron Spectroscopic Data. *J. Res. Natl. Inst. Stand. Technol.* **2009**, *114*, 341−358.
(36) Jouault, N.; Crawford, M. K.; Chi, C.; Smalley, R. J.; Wood, B.; Jestin, J.; Melnichenko, Y. B.; He, L.; Guise, W. E.; Kumar, S. K. Polymer Chain Behavior in Polymer Nanocomposites with Attractive Interactions. *ACS Macro Lett.* **2016**, *5*, 523−527.
(37) Guinier, A.; Fournet, G. *Small-Angle Scattering of X-Rays*; John Wiley and Sons: New York, 1955.
(38) Hayter, J. B.; Penfold, J. An analytic structure factor for macroion solutions. *Mol. Phys.* **1981**, *42*, 109−118.
(39) Hansen, J.-P.; Hayter, J. B. A rescaled MSA structure factor for dilute charged colloidal dispersions. *Mol. Phys.* **1982**, *46*, 651−656.
(40) Oosawa, F.; Asakura, S. On Interaction between Two Bodies Immersed in a Solution of Macromolecules. *J. Chem. Phys.* **1954**, *22*, 1255−1256.
(41) Asakura, S.; Oosawa, F. Interaction between particles suspended in solutions of macromolecules. *J. Polym. Sci.* **1958**, *33*, 183−192.
(42) Lekkerkerker, H. N. W.; Poon, W. C.-K.; Pusey, P. N.; Stroobants, A.; Warren, P. B. Phase Behaviour of Colloid + Polymer Mixtures. *Europhys. Lett.* **1992**, *20*, 559−564.
(43) Tuinier, R.; Aarts, D. G. A. L.; Wensink, H. H.; Lekkerkerker, H. N. W. Pair interaction and phase separation in mixtures of colloids and excluded volume polymers. *Phys. Chem. Chem. Phys.* **2003**, *5*, 3707−3715.
(44) Lekkerkerker, H. N.; Tuinier, R. *Colloids and the Depletion Interaction*; Lecture Notes in Physics; Springer Netherlands: Dordrecht, 2011; Vol. *833*.
(45) Mildner, D. F. R.; Hall, P. L. Small-angle scattering from porous solids with fractal geometry. *J. Phys. D: Appl. Phys.* **1986**, *19*, 1535−1545.
(46) Teixeira, J. Small-angle scattering by fractal systems. *J. Appl. Crystallogr.* **1988**, *21*, 781−785.

DOI: 10.1021/acs.macromol.6b01277
Macromolecules 2016, 49, 6568−6577

(47) Lin, M. Y.; Lindsay, H. M.; Weitz, D. A.; Ball, R. C.; Klein, R.; Meakin, P. Universality in colloid aggregation. *Nature* **1989**, *339*, 360−362.
(48) Díez Orrite, S.; Stoll, S.; Schurtenberger, P. Off-lattice Monte Carlo simulations of irreversible and reversible aggregation processes. *Soft Matter* **2005**, *1*, 364−371.
(49) Liu, S.; Senses, E.; Jiao, Y.; Narayanan, S.; Akcora, P. Structure and Entanglement Factors on Dynamics of Polymer-Grafted Nanoparticles. *ACS Macro Lett.* **2016**, *5*, 569−573.
(50) Chatterjee, T.; Jackson, A.; Krishnamoorti, R. Hierarchical Structure of Carbon Nanotube Networks. *J. Am. Chem. Soc.* **2008**, *130*, 6934−6935.
(51) Huang, C. C.; Winkler, R. G.; Sutmann, G.; Gompper, G. Semidilute polymer solutions at equilibrium and under shear flow. *Macromolecules* **2010**, *43*, 10107−10116.
(52) Joanny, J. F.; Leibler, L.; De Gennes, P. G. Effects of polymer solutions on colloid stability. *J. Polym. Sci., Polym. Phys. Ed.* **1979**, *17*, 1073−1084.
(53) Fleer, G. J.; Skvortsov, A. M.; Tuinier, R. Mean-Field Equation for the Depletion Thickness. *Macromolecules* **2003**, *36*, 7857−7872.
(54) Karatrantos, A.; Composto, R. J.; Winey, K. I.; Kröger, M.; Clarke, N. Entanglements and Dynamics of Polymer Melts near a SWCNT. *Macromolecules* **2012**, *45*, 7274−7281.
(55) Glomann, T.; Hamm, A.; Allgaier, J.; Hübner, E. G.; Radulescu, A.; Farago, B.; Schneider, G. J. A microscopic view on the large scale chain dynamics in nanocomposites with attractive interactions. *Soft Matter* **2013**, *9*, 10559−10571.
(56) Glomann, T.; Schneider, G. J.; Allgaier, J.; Radulescu, A.; Lohstroh, W.; Farago, B.; Richter, D. Microscopic Dynamics of Polyethylene Glycol Chains Interacting with Silica Nanoparticles. *Phys. Rev. Lett.* **2013**, *110*, 178001.
(57) Ashkar, R.; Abdul Baki, M.; Tyagi, M.; Faraone, A.; Butler, P.; Krishnamoorti, R. Kinetic Polymer Arrest in Percolated SWNT Networks. *ACS Macro Lett.* **2014**, *3*, 1262−1265.
(58) Holt, A. P.; Griffin, P. J.; Bocharova, V.; Agapov, A. L.; Imel, A. E.; Dadmun, M. D.; Sangoro, J. R.; Sokolov, A. P. Dynamics at the Polymer/Nanoparticle Interface in Poly(2-vinylpyridine)/Silica Nanocomposites. *Macromolecules* **2014**, *47*, 1837−1843.
(59) Richter, D.; Binder, K.; Ewen, B.; Stuehn, B. Screening of hydrodynamic interactions in dense polymer solutions: a phenomenological theory and neutron-scattering investigations. *J. Phys. Chem.* **1984**, *88*, 6618−6633.
(60) Monkenbusch, M. In *Neutron Spin Echo Spectroscopy - Basics, Trends and Applications*; Mezei, F., Pappas, C., Gutberlet, T., Eds.; Springer: 2003; pp 246−265.
(61) Ahlrichs, P.; Everaers, R.; Dünweg, B. Screening of hydrodynamic interactions in semidilute polymer solutions: A computer simulation study. *Phys. Rev. E: Stat. Phys., Plasmas, Fluids, Relat. Interdiscip. Top.* **2001**, *64*, 040501.
(62) Smith, G. D.; Bedrov, D.; Li, L.; Byutner, O. A molecular dynamics simulation study of the viscoelastic properties of polymer nanocomposites. *J. Chem. Phys.* **2002**, *117*, 9478−9489.
(63) Schneider, G. J.; Nusser, K.; Neueder, S.; Brodeck, M.; Willner, L.; Farago, B.; Holderer, O.; Briels, W. J.; Richter, D. Anomalous chain diffusion in unentangled model polymer nanocomposites. *Soft Matter* **2013**, *9*, 4336−4348.
(64) Wang, B.; Anthony, S. M.; Bae, S. C.; Granick, S. Anomalous yet Brownian. *Proc. Natl. Acad. Sci. U. S. A.* **2009**, *106*, 15160−15164.
(65) Guo, H.; Bourret, G.; Lennox, R. B.; Sutton, M.; Harden, J. L.; Leheny, R. L. Entanglement-Controlled Subdiffusion of Nanoparticles within Concentrated Polymer Solutions. *Phys. Rev. Lett.* **2012**, *109*, 055901.
(66) Lin, Y. H. Number of entanglement strands per cubed tube diameter, a fundamental aspect of topological universality in polymer viscoelasticity. *Macromolecules* **1987**, *20*, 3080−3083.
(67) Segrè, P. N.; Behrend, O. P.; Pusey, P. N. Short-time Brownian motion in colloidal suspensions: Experiment and simulation. *Phys. Rev. E: Stat. Phys., Plasmas, Fluids, Relat. Interdiscip. Top.* **1995**, *52*, 5070−5083.
(68) Segrè, P. N.; Pusey, P. N. Scaling of the Dynamic Scattering Function of Concentrated Colloidal Suspensions. *Phys. Rev. Lett.* **1996**, *77*, 771−774.
(69) Sikorski, M.; Sandy, A. R.; Narayanan, S. Depletion-Induced Structure and Dynamics in Bimodal Colloidal Suspensions. *Phys. Rev. Lett.* **2011**, *106*, 188301.
(70) Hoshino, T.; Kikuchi, M.; Murakami, D.; Harada, Y.; Mitamura, K.; Ito, K.; Tanaka, Y.; Sasaki, S.; Takata, M.; Jinnai, H.; Takahara, A. X-ray photon correlation spectroscopy using a fast pixel array detector with a grid mask resolution enhancer. *J. Synchrotron Radiat.* **2012**, *19*, 988−993.
(71) Richter, D.; Farago, B.; Fetters, L. J.; Huang, J. S.; Ewen, B. On the relation between structure and dynamics of star polymers in dilute solution. *Macromolecules* **1990**, *23*, 1845−1856.
(72) Vlassopoulos, D.; Pakula, T.; Fytas, G.; Roovers, J.; Karatasos, K.; Hadjichristidis, N. Ordering and viscoelastic relaxation in multiarm star polymer melts. *Europhys. Lett.* **1997**, *39*, 617−622.
(73) Caronna, C.; Chushkin, Y.; Madsen, A.; Cupane, A. Dynamics of Nanoparticles in a Supercooled Liquid. *Phys. Rev. Lett.* **2008**, *100*, 055702.
(74) Lubchenko, V.; Wolynes, P. G. Theory of aging in structural glasses. *J. Chem. Phys.* **2004**, *121*, 2852−2865.
(75) Heuer, A. Exploring the potential energy landscape of glass-forming systems: from inherent structures via metabasins to macroscopic transport. *J. Phys.: Condens. Matter* **2008**, *20*, 373101.
(76) Hoy, R. S.; Grest, G. S. Entanglements of an End-Grafted Polymer Brush in a Polymeric Matrix. *Macromolecules* **2007**, *40*, 8389−8395.
(77) Martin, T. B.; Mongcopa, K. I. S.; Ashkar, R.; Butler, P.; Krishnamoorti, R.; Jayaraman, A. Wetting-Dewetting and Dispersion-Aggregation Transitions Are Distinct for Polymer Grafted Nanoparticles in Chemically Dissimilar Polymer Matrix. *J. Am. Chem. Soc.* **2015**, *137*, 10624−10631.
(78) Singh, R.; Lillard, J. W. Nanoparticle-based targeted drug delivery. *Exp. Mol. Pathol.* **2009**, *86*, 215−223.
(79) He, K.; Retterer, S. T.; Srijanto, B. R.; Conrad, J. C.; Krishnamoorti, R. Transport and Dispersion of Nanoparticles in Periodic Nanopost Arrays. *ACS Nano* **2014**, *8*, 4221−4227.
(80) Babayekhorasani, F.; Dunstan, D. E.; Krishnamoorti, R.; Conrad, J. C. Nanoparticle dispersion in disordered porous media with and without polymer additives. *Soft Matter* **2016**, *12*, 5676−5683.

DOI: 10.1021/acs.macromol.6b01277
Macromolecules 2016, 49, 6568−6577